Applied Energy 121 (2014) 1–9

Contents lists available at ScienceDirect

Applied Energy

journal homepage: www.elsevier.com/locate/apenergy

Understanding the chemical and structural transformations of lignin macromolecule during torrefaction

Jia-Long Wen [a], Shao-Long Sun [a], Tong-Qi Yuan [a], Feng Xu [a], Run-Cang Sun [a,b,*]

[a] *Beijing Key Laboratory of Lignocellulosic Chemistry, Beijing Forestry University, Beijing 100083, China*
[b] *State Key Laboratory of Pulp and Paper Engineering, South China University of Technology, Guangzhou 510640, China*

HIGHLIGHTS

- The terrified bamboo has a high energy yield of 85.7% and a HHV of 20.13 MJ/kg.
- The structural changes of hemicelluloses, cellulose, and lignin were investigated.
- First study on the structural transformations of lignin during torrefaction.
- The mechanism of structural changes of lignin has been proposed.

GRAPHICAL ABSTRACT

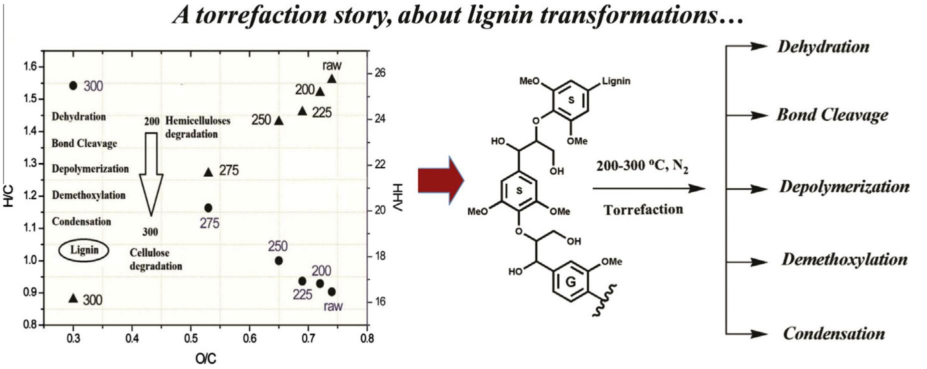

ARTICLE INFO

Article history:
Received 6 September 2013
Received in revised form 17 December 2013
Accepted 4 February 2014
Available online 19 February 2014

Keywords:
Bamboo
Bioenergy
Lignin
NMR
Structural transformations
Torrefaction

ABSTRACT

Torrefaction is an efficient method to recover energy from biomass. Herein, the characteristics (mass yield, energy yield, physical, and chemical characteristics) of torrefied bamboo at diverse temperatures (200–300 °C) were firstly evaluated by elemental analysis, XRD, and CP–MAS ^{13}C NMR methodologies. Under an optimal condition the terrified bamboo has a relative high energy yield of 85.7% and a HHV of 20.13 MJ/kg. The chemical and structural transformations of lignin induced by thermal treatment were thoroughly investigated by FT-IR and solution-state NMR techniques (quantitative ^{13}C NMR, 2D-HSQC, and ^{31}P-NMR methodologies). The results highlighted the chemical reactions of the native bamboo lignins towards severe torrefaction treatments occurred, such as depolymerization, demethoxylation, bond cleavage, and condensation reactions. NMR results indicated that aryl-ether bonds (β-*O*-4) and *p*-coumaric ester in lignin were cleaved during the torrefaction process at mild conditions. The severe treatments of bamboo (275 °C and 300 °C) induced a dramatic enrichment in lignin content together with the almost complete disappearance of β-*O*-4, β-β, and β-5 linkages. Further analysis of the molecular weight of milled wood lignin (MWL) indicated that the average molecular weights of "torrefied MWL" were lower than those of control MWL. It is believed that understanding of the reactivity and chemical transformations of lignin during torrefaction will contribute to the integrated torrefaction mechanism.

© 2014 Elsevier Ltd. All rights reserved.

1. Introduction

Bioenergy has been considered as one of attractive renewable energy alternatives in the future [1]. Among the existing technologies to enhance lignocellulosic biomass for renewable energy

---

* Corresponding author at: Beijing Key Laboratory of Lignocellulosic Chemistry, Beijing Forestry University, Beijing 100083, China. Tel./fax: +86 10 62336903.
E-mail address: rcsun3@bjfu.edu.cn (R.-C. Sun).

http://dx.doi.org/10.1016/j.apenergy.2014.02.001
0306-2619/© 2014 Elsevier Ltd. All rights reserved.

production, torrefaction was regarded as a simple and efficient method. Torrefaction is a thermo-chemistry process that enables energy densification of biomass and biomass homogenization, which usually conducted in an inert atmosphere and low temperatures of 200–300 °C [2]. In fact, the basic principle of torrefaction is the removal of oxygen and enrichment of carbon of the final solid product. The torrefied biomass has a lower O/C ratio as compared to the original biomass [2]. Besides, the torrefied biomass has a higher energy density and grindability, which enhance the combustion performance. Due to the aforementioned advantages of torrefaction, research and development activities in biomass torrefaction for energy applications worldwide were very active in these years [3–15].

Up to now, different methods and various feedstock types employed in torrefaction have been reported [3–15]. Among the existing feedstocks employed for torrefaction, bamboo will be an excellent feedstock for future torrefaction industry [11]. Bamboo is a promising biomass for future energy production because of its high growth rate and a number of major fuel characteristics, such as low ash content and high heating value [16]. Bamboo species widely distributed in Asian countries and their traditional applications are well known. Nevertheless, it is of great importance to use efficient biomass conversion technologies to take advantage of bamboo's characteristics (high contents of cellulose and lignin) under the context of biomass utilization [11].

Torrefaction is a thermochemistry process, which not only removes water and low molecular-weight organic volatile components, but also induces chemical transformations of the polymers in the plant cell wall, and thus affects the mechanical strength of the material [15]. For example, the major components in biomass (cellulose, hemicelluloses, and lignin macromolecules) are variously affected by torrefaction process, depending on their respective chemical reactivity. Although most researches focus on the physical characteristics (mass yield, ultimate analyses, and grindability) of the torrefied biomass, however, as a very important issue, the chemical and structural transformations of components in biomass have not been thoroughly understood during torrefaction process.

Lignocellulosic biomass is a natural bio-composite, mainly formed by cellulose, hemicelluloses, and lignin. The transformations of chemical and structural features during torrefaction process have a direct influence on the quality of the final product. Lignins are complex natural polymers with various phenolic structures, which significantly affect the final properties of the torrefied bimass. The native lignins of bamboo (*Phyllostachys*) are essentially composed of *p*-hydroxyphenyl (H, 1–2%), guaiacyl (G, 21–31%), and syringyl (S, 67–78%) units associated with abundant *p*-coumarates and ferulates [17]. The main substructures of native lignins are the aryl ether bonds (β-*O*-4 linkages), which are mainly composed of S-type lignin units, while the proportion of carbon–carbon bonds in native lignins is less. It was reported that the lignin degradation starts at temperatures above 200 °C, with a slower kinetics than that of the hemicelluloses degradation [18]. The effect of severe thermal treatment (220–280 °C) on spruce and beech wood lignins has been investigated by thioacidolysis method [19]; however, the understanding of the composition and structure of the lignin macromolecule is traditionally conducted by wet chemical methods, such as thioacidolysis (TA), nitrobenzene oxidation (NBO), and derivatization followed by reductive cleavage (DFRC). These methods are effective in analyzing "native lignin" in plant cell wall. However, they will be ineffective when investigating the structurally changed lignin because that they only considering the ether linkages, but not regarding the changes of carbon–carbon bonds in lignin. Thanks to recent advances in nuclear magnetic resonance (NMR), our knowledge of this natural polymer has been improved and expanded [20–22]. Most of the ether linkages (β-*O*-4 ones) were expected to be cleaved at 200–350 °C via thermal analysis [23]. However, the reactivity and chemical transformations of lignins during torrefaction have been less studied and poorly understood. As a method for upgrading biomass for fuels, it is desired to obtain more solid with lower O/C ratios during torrefaction. Therefore, it is expected that the structural evolution of lignin macromolecule could provide indications for optimizing the torrefaction conditions and hence improve the quality of torrefied biomass.

In the present study, the torrefied bamboo samples under different conditions have been investigated by component analysis, elemental analysis, energy yield, XRD, and CP–MAS ^{13}C NMR techniques. In addition, milled wood lignin (MWL), which is considered to be an ideal representative of "native lignin", extracted from the control and torrefied bamboo and thoroughly analyzed using FT-IR spectra, quantitative ^{13}C NMR, 2D-HSQC NMR, and ^{31}P NMR spectra. Moreover, gel permeation chromatography (GPC) was also used to investigate the effects of torrefaction temperatures on the molecular weight of the lignins. It is believed that the effects of different torrefaction temperatures on the lignin macromolecules and the concomitant chemical transformation of lignin could be observed in a resolved and observable manner.

2. Experimental

2.1. Material

Bamboo (*Phyllostachys pubescens*) was obtained from Shangrao, Jiangxi, China. The culms were manually separated before dried at 50 °C, and the particles with a size between 450 and 900 μm (20–40 mesh) were collected. The dewaxed material (toluene/ethanol, 2:1, v/v; Soxhlet extractor; 12 h) was dried at 60 °C for 16 h.

2.2. Torrefaction process

The torrefaction of bamboo was conducted in a tubular furnace (Furnace 1200C, Central furnace, Tianjin, China). After drying of the bamboo particles in an oven at 105 °C for 24 h as a pre-treatment process, in which the moisture was completely eliminated, the dried samples were put into sample box of furnace. For every torrefaction experiment, a feedstock amount of 25 g of bamboo was used. The feedstock was placed in the sample cup, which was then mounted to the inner cylinder of the reactor. The bamboo was torrefied at 200, 225, 250, 275, and 300 °C for 1 h in the absence of oxygen, respectively. The flow rate of nitrogen was 0.5 L/min. The reaction was processed in two stages. In the first stage, the temperature was risen up to the required torrefied temperature in a desired time (40–60 min, 5 °C/min); in the second stage, the bamboo sample stayed at setting torrefied temperature for the setting residence time (60 min). After torrefaction, the torrefied bamboo samples were collected and weighed.

2.3. "Milled wood lignin" from torrefaction biomass

The crude "milled wood lignin, (MWL)" sample was prepared from bamboo according to classic procedures [24]. The ball-milled of bamboo (control and torrefied bamboo) was prepared with a planetary ball mill for 2 h as previously reported [25].

2.4. Physicochemical characterization of the torrefied bamboo

The compositions of the polysaccharides and lignin in the torrefied bamboo samples were analyzed using the Laboratory Analytical Procedure (LAP) for biomass provided by the NREL [26]. Elemental analysis (C, H, and O) was carried out in an elemental analyzer Vario EL III (Elementar, Hanau, Germany) [17]. The high heating value (HHV) of the sample was calculated on the basis of Dulong's formula according to Liu et al. (2012) [27],

$$\text{HHV(MJ/kg)} = 0.3383\ \text{C} + 1.442(\text{H—O}/8)$$

in which C, H, and O represent the weight percentages of carbon, hydrogen, and oxygen, respectively.

$$\text{EY (\%)} = \text{mass yield} \times \text{HHV (torrefied sample)}/\text{HHV (raw sample)} \times 100\%$$

The crystallinities of the control and torrefied bamboo were measured using an XRD-6000 instrument (Shimadzu, Japan) [28]. Solid-state cross-polarization/magic angle spinning (CP/MAS) ^{13}C NMR spectra of the samples were obtained using a Bruker AVIII 400 M spectrometer (Bruker, Germany) [28].

2.5. Characterization of MWL samples from control and torrefied bamboo

FT-IR spectra of lignin preparations were obtained using a Thermo Scientific Nicolet iN10 FT-IR microscope (Thermo Nicolet Corp., Madison, WI, USA) [25]. The molecular weights of the lignin were determined by GPC as previously reported [25]. NMR spectra were recorded on a Bruker AVIII 400 MHz spectrometer at 25 °C in DMSO-d_6. The quantitative ^{13}C NMR and quantitative 2D-HSQC experiments were conducted according to a previous literature [29]. ^{31}P NMR spectra were acquired according to a previous literature [30].

3. Results and discussion

3.1. Mass yield, elemental analysis, energy yield, and component analysis

The mass yield, klason lignin content, elemental analysis, high heating values (HHV), energy yield, and component analysis of the control and torrefied bamboo are listed in Table 1. The yield of torrefied bamboo was directly affected by torrefaction temperature. As the torrefaction temperature increased from 200 to 300 °C, the yield of the torrefied bamboo decreased gradually from 92.3% to 47.0%. The mass loss of bamboo during torrefaction was primarily due to the decomposition of hemicelluloses and partly because of the depolymerization of cellulose and lignin [31], as also revealed by the component analysis of the torrefied bamboo samples (Table 1). It was observed that the degradation of hemicelluloses began at 200 °C, while the degradation of cellulose occurred when the temperature above 250 °C. The effect of the torrefaction on the klason lignin content of bamboo is listed in Table 1. The klason lignin content in the torrefied bamboo increased with the severity of the thermal treatment, reaching a very high value (97.1%) in the sample treated for 1 h at 300 °C. This result suggested that the cell wall polysaccharides were mostly eliminated, and the lignin content was overestimated by the klason method because such treatment induced some recondensation reactions between polysaccharides (or polysaccharide degradation products) and lignin, which was also called "Pseudo-lignin" [32]. The elemental analysis results of the torrefied bamboo are also shown in Table 1. It is evident that the carbon content increased significantly with elevating temperature, whereas the oxygen content decreased accordingly. Therefore, the O/C ratio of the torrefied bamboo decreased with elevated temperature, suggesting that deoxygenation of bamboo is the primary reactions during torrefaction. Results from the elemental analysis are plotted on a van Krevelen diagram in Fig. 1 (H/C, O/C, and HHV). The observed tendency agrees with other data from a previous literature [15]. HHV results indicated that the torrefied bamboo has a higher HHV than the original bamboo. Compared to the HHV (16.46 MJ/kg) of the control bamboo (dried at 105 °C, 24 h), the HHV of torrefied bamboo (25.48 and 20.13 MJ/kg) increased by 55% after torrefaction at 300 °C for 1 h and increased by 22% after torrefaction at 275 °C for 1 h, which was close to the HHV of charcoal and peat, respectively [2]. In addition, the torrefaction led to an increase of the carbon content and to a decrease of both the hydrogen and the oxygen contents. It was also found that a gap between the HHV of the bamboo samples torrefied at 300 °C and those treated at lower temperatures (200–275 °C), which was in agreement with the evolution of the mass losses as a function of the treatment temperatures (Fig. 1). The O/C and H/C ratios for the torrefied bamboo at 300 °C were 0.88 and 0.30, respectively, near to those of charcoal and coal [2]. However, the mass yield was only 47.0% and the corresponding energy yield was 72.7% of the initial energy content (control sample). The mass and energy yields are the most important parameters in evaluating torrefaction of bamboo. An optimal balance of mass and energy for biomass torrefaction is as follows: 70% of the mass is retained as a solid product, containing 90% of the initial energy content; while the other 30% of the mass is converted into torrefaction gas, only equaling to 10% of the energy of the biomass [2]. In this study, the energy yield decreased with mass yield, reached to 85.7% of initial energy content at 275 °C, while the mass yield is 70.1% at this temperature. The O/C and H/C ratios of the torrefied bamboo at 275 °C were similar to those of peat [2]. The results highlighted the demand for optimization of the torrefaction

Table 1
Mass yields, component analysis, elemental analysis, and energy yield of torrefied bamboo at different temperatures (200–300 °C).

	Control	200	225	250	275	300
MY (%)[a]	100	92.3	90.0	82.4	70.1	47.0
C (%)	47.24	48.05	48.84	50.30	55.25	68.14
H (%)	6.16	6.12	5.93	6.02	5.86	5.04
O (%)	46.60	45.83	45.23	43.68	38.89	26.82
O/C ratio	0.74	0.72	0.69	0.65	0.53	0.30
H/C ratio	1.56	1.52	1.46	1.43	1.27	0.88
HHV[b]	16.46	16.82	16.93	17.82	20.13	25.48
EY (%)[c]	100.0	94.3	92.6	89.2	85.7	72.7
KL (%)[d]	26.7	27.0	30.4	32.3	53.1	97.1
Glucan	40.0	45.8	48.7	50.9	42.6	1.9
Xylan	29.0	22.2	19.7	10.7	4.0	0.1

[a] MY, mass yield.
[b] HHV, high heating value.
[c] EY, energy yield.
[d] KL, klason lignin.

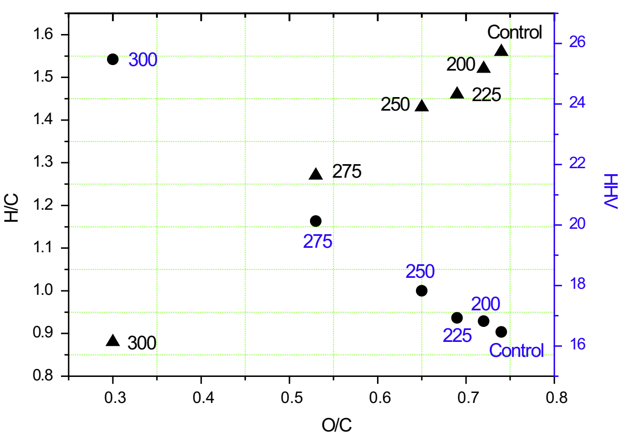

Fig. 1. Van Krevelen diagram of the control and torrefied bamboo.

conditions used is urgent, which will result in the final fuel quality. As a whole, within the investigated ranges of torrefaction temperatures, over 70% of energy yield can be obtained from the torrefaction. However, considering the mass yield, energy yield in this study based on the optimal balance of mass and energy, it was concluded that torrefaction at 275 °C for 1 h was the optimal condition.

3.2. XRD analysis

To understand the effects of torrefaction on the crystallinity of the bamboo, the crystallinity index (CrI) for all samples was calculated from the XRD data, and the results and the XRD patterns are shown in Fig. 2. As can be seen, the control bamboo had a CrI of 41.57%, and after torrefaction at 200 °C, it was found that there was a small decrease in the CrI (40.01%). This decrease in CrI suggested that parts of hydrogen bonds in bamboo were broke down slightly after torrefaction. However, the CrI of the torrefied bamboo increased to 42.93% when the temperature increased to 225 °C, which was probably due to the degradation of hemicelluloses at this temperature. In addition, the initially increased CrI also suggested that amorphous (or disordered) cellulose was partly recrystallized due to thermal treatment (200–225 °C), before being degraded at higher temperatures (250–300 °C) [15]. As the temperature further increased from 250 to 275 °C, the CrI began to decrease continuously as result of the degradation of crystalline cellulose at higher temperatures. With the temperature further increased to 300 °C, the pattern presented a distinctive shape and the corresponding CrI sharply reduced to 30.43%. The decreased CrI was mostly attributed to the degradation of the crystalline cellulose.

3.3. CP–MAS ^{13}C NMR spectra

CP–MAS ^{13}C NMR spectra (Fig. 3) were used to investigate the structural changes between these bamboo samples. For control bamboo, the signals at 172.6 and 20.7 ppm are predominantly assigned to the acetyl group of hemicelluloses. In addition, all noticeable signals were distributed in the region between 50.0 and 110.0 ppm for the carbons of carbohydrate polymers [28,33]. The overlapping signals from C-2, C-3, and C-5 of carbohydrate polymers exhibited a strong signal at about 73.0 ppm. The signals for lignin polymer were observed at 152.6, 147.6, 133.2, 121.6, 114.2, and 55.0 ppm, which are represented for $S_{3,5}$ (etherified), $S_{3,5}$ (non-etherified), S_1/S_4(non-etherified), G_6, G_5, and OCH_3 in lignin, respectively [33]. After torrefaction at different temperatures, the spectra of the torrefied bamboo presented slightly different patterns. The most striking feature of these spectra was the signals located at 152.6 and 147.6 ppm. The signal from etherified $S_{3,5}$ (152.6 ppm) decreased while that from non-etherified $S_{3,5}$ (147.6 ppm) increased, suggesting that β-*O*-4 linkages began to degrade at 225 °C. The degradation of β-*O*-4 structures was severe with the increased temperature, and the signals (23.0 and 172.0 ppm) of hemicelluloses significantly reduced and disappeared at higher temperatures (250–300 °C). Compared to lignin and hemicelluloses, cellulose seems to be stable under the torrefaction temperatures (200–275 °C). The crystalline index (CrI) calculated from CP–MAS ^{13}C NMR spectra of raw bamboo was 0.33, while it decreased to 0.27 as the temperature increased to 200 °C, implying that parts of hydrogen bonds in bamboo were broken down slightly after torrefaction. The result was in agreement with the analysis of XRD patterns. As the temperature further increased from 225 °C to 275 °C, the CrI increased from 0.30 to 0.36, suggesting that most amorphous substances (hemicelluloses and amorphous cellulose) were degraded at the temperature range, which was in agreement with a recent publication [12]. However, as the temperature increased to 300 °C, the NMR spectrum of the torrefied bamboo differs markedly from those obtained at other temperatures (200–275 °C). Indeed, all the signals assigned to cellulose decreased drastically, the disappeared C-4 and C-6 signals in cellulose were probably attributed to depolymerization and charring [15]. After torrefaction at 300 °C for 1 h, the cellulose and hemicelluloses in the bamboo were mostly degraded. The residue contains enriched amounts of carbonyl groups (177.0 ppm), aromatic carbons (146.1, 127.1, and 104.2 ppm) and methoxyl groups (54.0 ppm), which represented complex condensed aromatics. These aromatics units were also linked with aliphatic C—O (60.0–100.0 ppm) and C—C bonds (10.0–20.0 ppm) [34]. Furthermore, new broad aromatic region at 110.0–160.0 ppm, which is due to an increase in aromatic carbon content, indicating charring of hemicelluloses, cellulose, and lignin at 300 °C for 1 h [15].

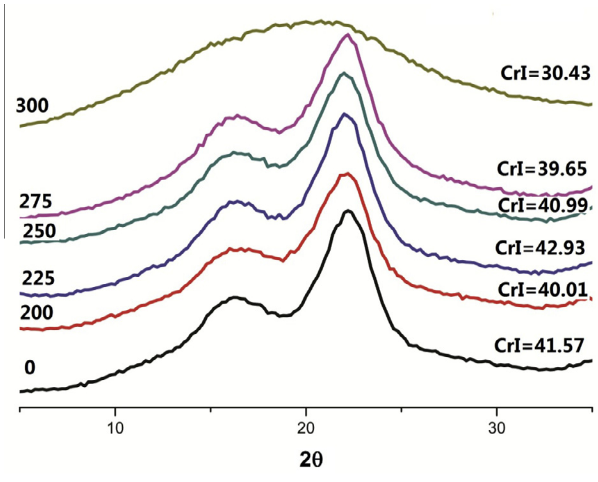

Fig. 2. XRD patterns of the control and torrefied bamboo samples.

3.4. FT-IR spectra of lignin

The FT-IR spectra of the lignin fractions isolated from the control and torrefied bamboo samples are shown in Fig. S1 (Supporting information) and the bands were assigned according to previous literatures [17,35]. It was observed that all spectra showed similar spectral patterns except for different intensities of infrared absorptions. The most typical bands (1600, 1510, and 1460 cm^{-1}) represent for aromatic regions of lignin decreased with increased temperatures, implying that aromatic rings began to degrade at higher temperatures. The intensity of the bands at 1422 and 1327 cm^{-1} decreased from 250 to 300 °C, suggesting that S-type lignin units began to degrade at 250 °C. The signal at 1164 cm^{-1}, which is represented for C=O in ester groups of HGS lignin, also gradually decreased at 200 °C and disappeared at 250 °C, suggesting that esterified *p*-coumaric acid was mostly cleaved at 250 °C. In addition, the intensity of the band at 1029 cm^{-1} (aromatic C—H in-plane deformation) started to decrease at 250 °C, implying that condensation reactions probably impeded the in-plane deformation of aromatic C—H. The tendency was in line with the reduced band at 1226 cm^{-1} (C—C, C—O, and C=O stretch), which is also indicated the condensation of G units. Moreover, the bonds at 1124 and 833 cm^{-1} began to reduce greatly at 250 °C, which further suggested that S units started to degrade at this temperature. However, the distinct evolution of lignin structures still needs to be supported by NMR spectral data.

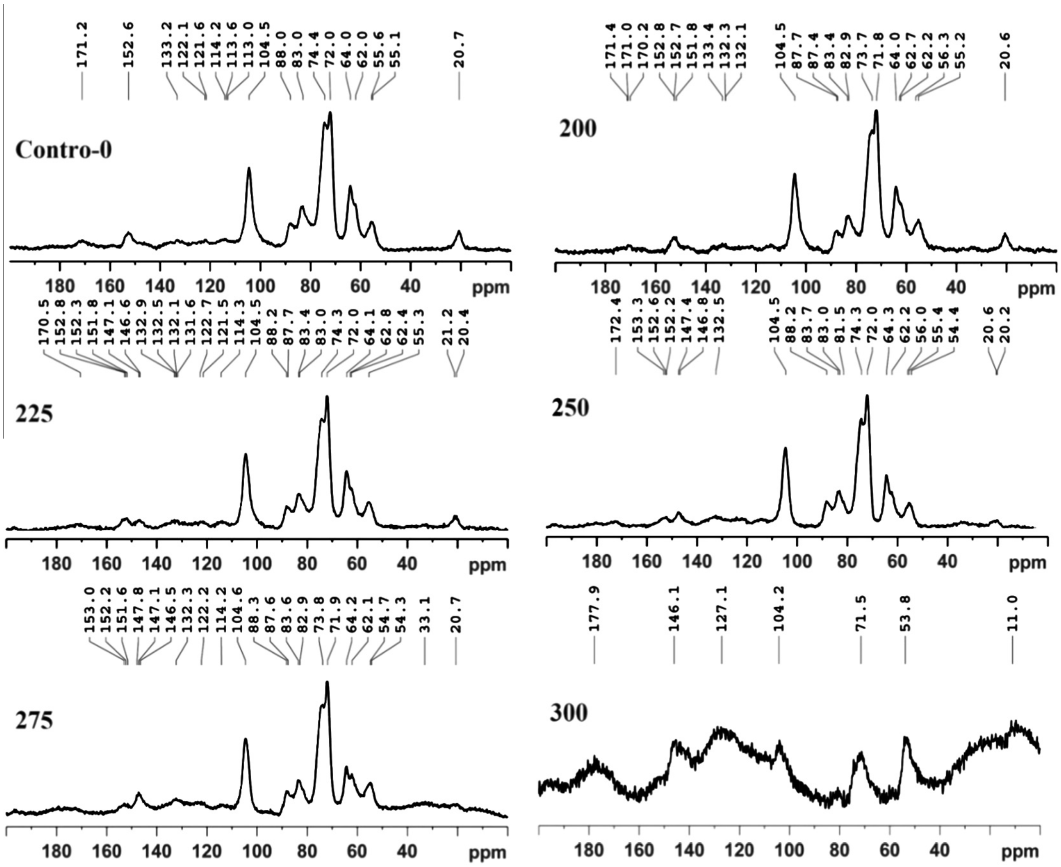

Fig. 3. CP–MAS ^{13}C spectra of the control and torrefied bamboo.

3.5. Quantitative ^{13}C NMR spectra of lignin

The quantitative ^{13}C NMR spectra of MWL samples are presented in Fig. 4. In the control MWL, *p*-coumaric acid is esterified (*in vivo p*-CE) to γ-position of the lignin polymers, as confirmed by the obvious signals at 166.5, 160.0, 144.7, 130.3, 125.1, 116.0, and 115.0 ppm, derived from C_9, C_4, C_7, C_2/C_6, C_1, C_3/C_5, and C_8 in *p*-coumaric ester (*p*-CE), respectively [17]. Apart from the signals represented for *p*-CE, the S, G, and H units in non-acetylated MWL are also clearly distinguished according to some publications [17,21,36]. After the torrefaction process, the MWL samples of the torrefied bamboo (225 and 275 °C) were used to investigate the detailed structural changes of lignin during the torrefaction process. Compared 225-MWL with control-MWL, it was found that most signals were similar except for some differences as follows: (1) The subdued signals for *p*-CE were probably due to the cleavage of the hanging molecules (*p*-CE); (2) The signals for β-*O*-4 linkages and etherified $S_{3,5}$ reduced and the signals for non-etherified G_3 and $S_{3/5}$ increased, suggesting that some β-*O*-4 linkages were cleaved and degraded at this temperature; (3) Shift of $S_{2,6}$ correlated signals to enlarged correlations (from 103.0 to 106.0 ppm) suggested that condensation involved in torrefaction process. By contrast, it was found that the signals for etherified $S_{3,5}$ (152.2 ppm), *p*-coumarate, normal $S_{2,6}$ (103.7 ppm) and β-*O*-4 linkages (60.2, 72.4, and 86.1 ppm) mostly disappeared in the spectrum in 275-MWL. Considering the increasing intensity of the signal at ~148.0 ppm (non-etherified $S_{3,5}$ and G_3), it was concluded that the ether bonds in β-*O*-4 linkages were mostly cleaved and transformed into non-etherfied $S_{3,5}$ or G_3 during the torrefaction.

Quantitative ^{13}C NMR spectra can be used to investigate detailed structural changes of lignin during torrefaction. For example, a comparison of the integration values of different regions can provide valuable information on the degree of condensation of the lignin fractions [29]. As shown in Fig. 4, the increase of torrefaction temperature resulted in an increase in integration of condensed aromatic carbons. In other words, this observation indicated an increasing degree of lignin condensation at a higher torrefaction temperature. It was also revealed that the cleavage of ether bonds (β-*O*-4 linkages) in lignin during the torrefaction will result in the recondensation of the radical to form aromatic carbon–carbon (C—C) bonds. The aliphatic region (89.0–58.0 ppm) of the ^{13}C NMR spectra displays signals arising from the aliphatic C—O on the lignin propyl side chain. It appears that an increase in torrefaction temperature resulted in a strong decrease of the aliphatic C—O signals from 1.94 per aryl group in control-MWL to 1.16 in 225-MWL, and further to 0.28 in 275-MWL. The fact suggested that the aliphatic C—O linkages (mainly β-*O*-4 linkages) in these lignin fractions were greatly cleaved and depolymerized as the temperature elevated.

3.6. 2D-HSQC NMR spectra of lignin

2D-HSQC NMR provides important structural transformations of the lignin during torrefaction. The information of substructures could be obtained by assigning the signals and quantifying of S/G ratio according to previous publications [17,20–21]. In the control MWL, the substructures, such as β-*O*-4 aryl ethers (A/A′), α-oxidized β-*O*-4 aryl ethers (A″), resinols (B), phenylcoumarans (C), spirodienones (D), non-acylated and acylated *p*-hydroxycinnamyl alcohol end-groups (I/I′), could be assigned according to a previous publication [17] and are depicted in Fig. S2 (Supporting information). As shown in Fig. 5, some substructures, such as

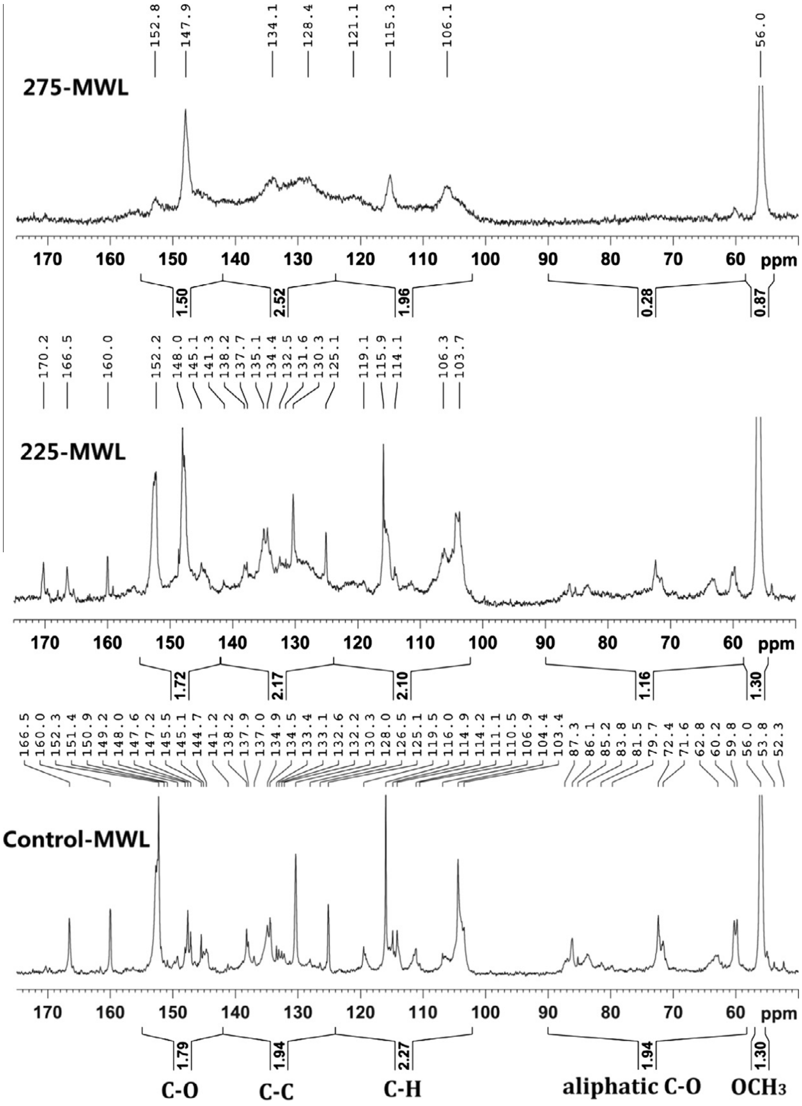

Fig. 4. Quantitative ^{13}C spectra of MWL from the control and torrefied bamboo.

spirodienones and *p*-hydroxycinnamyl alcohol end-groups, disappeared in the spectra of 200-MWL and 225-MWL after torrefaction at 200 °C and 225 °C for 1 h, while the *in vitro* acetylation probably occurred during torrefaction at these temperatures, as revealed by the elevated signals at γ-position of β-*O*-4 aryl ethers (A'_γ) and β position of G/H-type and S-type β-*O*-4 aryl ethers ($A_{\beta(G/H)'}$ and $A_{\beta(G/H)}$). The increased signals suggested that acetylation process mainly occurred at γ-position of β-*O*-4 linkages. The origin of acetylation is probably attributed to the released acetic acid during initial stage of torrefaction [12]. It was found that the signals for all the detected linkages were decreased and the reduced signals suggested that most linkages were cleaved at higher temperatures (above 250 °C). As the temperature increased to 275 and 300 °C, none linkages (Fig. 5) were observed except for the signals at 60.0/3.70 ppm and 55.0/3.70 ppm, which were probably due to the oxygenated carbon and OCH_3 in lignin, respectively. Combined with the aforementioned ^{13}C—NMR spectrum of 275-MWL, it was possible to conclude most of β-*O*-4 linkages was cleaved, meanwhile, minor linkages, such as β-β and β-5 were also disappeared in the spectra of MWLs extracted from torrefied bamboo at 275 and 300 °C. The aromatic region of 2D-HSQC spectra (Fig. 6) showed the basic compositions of lignin macromolecules, such as G, S, and H units. In addition, linked hydroxycinnamic acid (mainly *p*-coumarates, PCE) was also observed in the control MWL and the chemical shifts of the assignments are listed in Table S1. The changes of aromatic information can trace the structural evolution of lignin during the torrefied temperatures from 200 to 300 °C. It was found that the MWL samples from the torrefied bamboo at lower temperatures (200 and 225 °C) exhibited similar spectra as that from control bamboo except for some condensed lignin units. However, when the temperature increased to 250 and 275 °C, it was observed that the signals of PCE_7 and PCE_8 disappeared, suggesting that PCE was mostly cleaved during torrefaction. As the temperature further increased to 300 °C, signals for S and G-type sharply decreased. The relative content of *p*-hydroxyphenyl units (no OCH_3) increased from 250–300 °C, suggesting that demethoxylation mainly occurred at higher temperatures.

Quantification of the lignin fractions by 2D-HSQC NMR method can provide explicit structural evolution during torrefaction at different temperatures [21]. As shown in Table 2, the relative content of β-*O*-4 linkage in control-MWL was 90.4%, while it was reduced to 84.6% in 200-MWL and 74.8% in 225-MWL, respectively. The results suggested that the linkages were cleaved to some extent during torrefaction at mild temperatures. The relative contents of other linkages, such as β-β and β-5, were steadily increased with the elevated temperatures and reached to 18.8% and 6.4% at

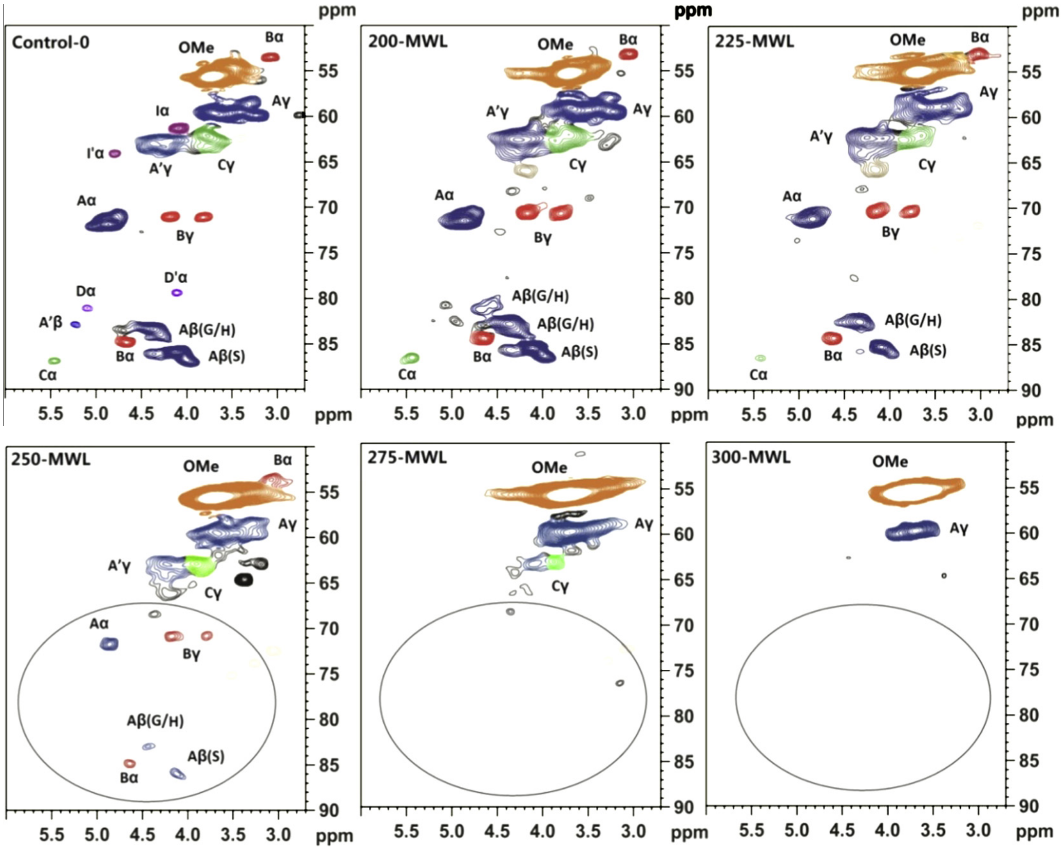

Fig. 5. 2D-HSQC spectra of MWL from the control and torrefied bamboo (side-chain region).

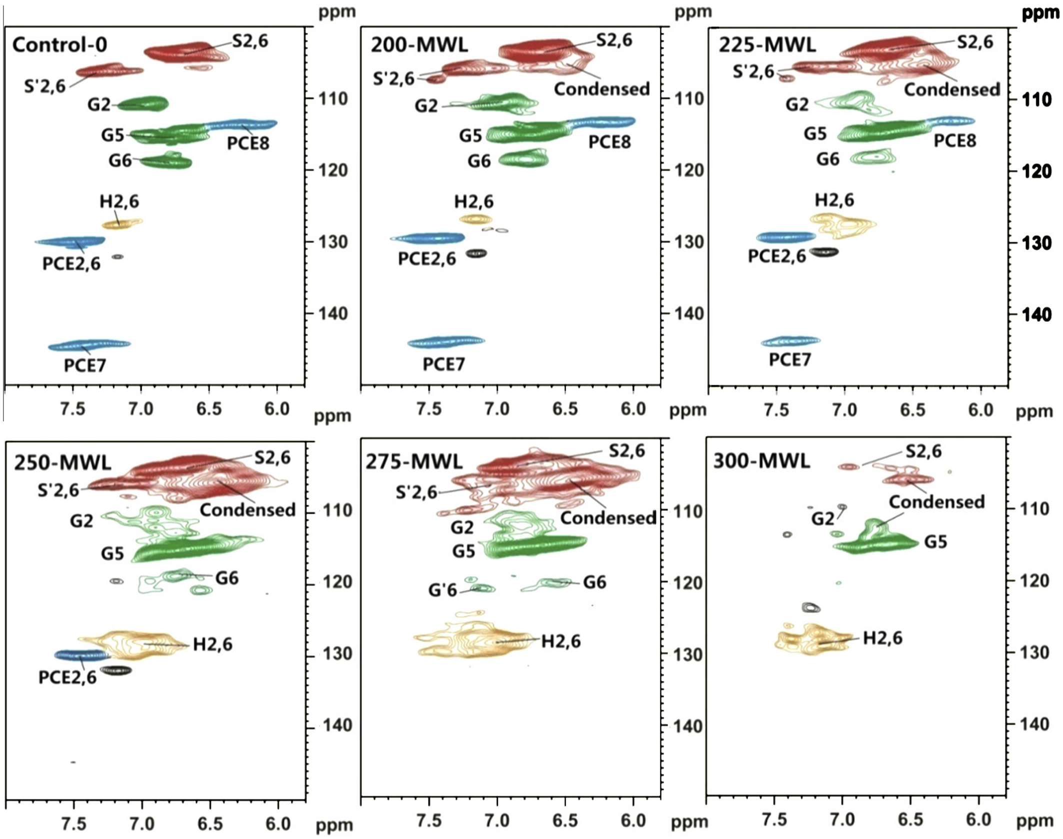

Fig. 6. 2D-HSQC spectra of MWL from the control and torrefied bamboo (aromatic region).

Table 2
Quantification of the MWL fractions by 2D-HSQC NMR spectra.

Sample	β-*O*-4	β-β	β-5	S/G/H	PCE
Control-MWL	90.4	8.4	1.2	68/30/2	32.7%
200-MWL	84.6	12.3	3.1	75/23/2	23.3%
225-MWL	74.8	18.8	6.4	73/17/10	12.3%
250-MWL	62.3	26.4	11.3	64/24/12	4.4%
275-MWL	N.D[a]	N.D	N.D	69/14/17	N.D
300-MWL	N.D	N.D	N.D	38/16/46	N.D

[a] N.D = not detected.

225 °C, respectively. The relative content of β-β and β-5 further increased to 26.4% and 11.3% at 250 °C, while the content of β-*O*-4 linkage relatively decreased to 62.3%. Another important parameter, S/G/H ratio, was also calculated to trace the changes of lignin composition. The S/G/H ratio of control MWL was 68/30/2, while it was increased to 75/23/2 in 200-MWL. This implied that some condensation reactions occurred preferably at G units and thus resulted in the suppression of G units in 2D-HSQC spectra, while H units remain stable at this temperature. With the torrefied temperature further increased to 225 °C, the relative content of G further decreased while H units increased to 10%, suggesting that part of G units began to transform into H units as a result of demethoxylation. As the temperature further increased to 250 °C, the relative content of S decreased, suggesting demethoxylation probably occurred in S units and part of S units began to transform into G units. When the temperature further increased to 275 °C, the relative content of G decreased while H increased, revealing that demethoxylation occurred in both S and G and the rate of demethoxylation was probably faster in S than G at higher temperatures. At 300 °C, the relative content of S units greatly decreased while H content sharply increased. This fact implied that most of S and G units have been transformed into H units at severe temperature. Besides the changes of relative content of linkages and S/G/H ratios, the PCE content in the MWL samples was also decreased with the elevated temperatures. For example, the PCE in control-MWL was 32.7% (based on $S_{2,6}/2 + G_2$), while it was reduced to 23.3% and 12.3% for 200-MWL and 225-MWL, respectively. Interestingly, the fact that the signals for PCE_7 and PCE_8 in 2D-HSQC spectra greatly reduced while the $PCE_{2,6}$ remained stable in MWL-250, which suggested that side-chain (position 7, 8, and 9) of PCE was cleaved. When the temperature rose to 275 and 300 °C, no signals from PCE were detected, implying that PCE were most cleaved at 250 °C or disappeared at higher temperatures.

3.7. ^{31}P NMR spectra of lignin

To further investigate the effects of torrefaction temperatures on the functional groups of the lignin in the torrefied bamboo, the MWL samples were comparatively studied by quantitative ^{31}P NMR techniques (*Fig.* S3). The aliphatic OH, condensed and uncondensed OH, and carboxylic acids were determined [30,37–38]. As shown in Table 3, the content of aliphatic OH gradually reduced as temperature increased, suggesting that the hydroxyl groups in the side-chain of lignin were fragmented and eliminated during torrefaction process. The γ-hydroxymethyl groups of lignin side-chains were found to be released in the form of formaldehyde, leading to the formation of resistant vinyl ether structures [19]. Besides the aliphatic OH, the contents of S and G-type phenolic hydroxyl groups greatly increased from control-MWL to 275-MWL, and the increasing rate of S was faster than that of G-type phenolic hydroxyl. However, the content of phenolic hydroxyl groups in S-type lignin was more than G-type lignin units. In short, the increase of phenolic hydroxyl groups was probably because of the cleavage of β-*O*-4 linkages, which has also been reported in a previous publication [39]. In addition, the content of S-type phenolic OH was higher than G-type phenolic OH in all the torrefied bamboo MWL samples, which suggested that most of the cleaved β-*O*-4 linkages are composed of S units. However, the content of S-type phenolic hydroxyl groups is decreased, which was due to the faster rate of demethoxylation in S-type unit than in G-type lignin at higher temperature (e.g. 300 °C). This was in agreement with 2D-HSQC results aforementioned. As a result of demethoxylation, the content of H-type phenolic hydroxyl slowly increased from 0.11 to 0.48 mmol/g (200–300 °C). By contrast, the content of phenolic hydroxyl in PCE molecules decreased greatly from 0.89 to 0 mmol/g (0–275 °C), which was in line with the analysis of the corresponding 2D-HSQC spectra. Moreover, there was no significant difference in the content of carboxyl groups among these samples, suggesting that oxidation was not a main reaction during the torrefaction. Furthermore, 2D-HSQC spectra of MWL samples revealed that some condensed lignin units appeared in the torrefied bamboo samples, the condensed S and G-type phenolic hydroxyl group also confirmed that condensation became more serious at higher temperatures (above 250 °C).

Table 3
Quantification of the MWL fractions by quantitative ^{31}P-NMR method (mmol/g).

Hydroxyl groups	Control	200	225	250	275	300
Aliphatic OH	4.14	3.33	1.78	1.06	0.50	0.35
C—S—OH[a]	0.01	0.02	0.15	0.28	0.31	0.27
NC—S—OH[b]	0.27	0.52	1.05	1.16	1.22	0.72
C—G—OH	0.08	0.11	0.23	0.27	0.30	0.24
NC—G—OH	0.43	0.42	0.54	0.57	0.71	0.81
NC—H—OH	N.D[c]	0.11	0.23	0.24	0.44	0.48
PCE—OH	0.89	0.67	0.46	0.23	N.D	N.D
COOH	0.08	0.04	0.05	0.11	0.08	0.12

[a] C, condensed.
[b] NC, non-condensed.
[c] N.D = not detected.

Table 4
Weight-average molecular weights (M_w), number-average (M_n) molecular weights, and polydispersity index (M_w/M_n) of the MWL fractions.

	Control	200	225	250	275	300
M_w	6080	2730	2410	2730	2130	1560
M_n	3230	1820	1550	1700	1200	980
M_w/M_n	1.88	1.50	1.56	1.60	1.77	1.59

3.8. Molecular weights

Table 4 showed the effects of torrefaction on the molecular weights of the lignin extracted from the torrefied bamboo. The M_w of the MWL from the control bamboo was 6080 g/mol, and it decreased to 2730–2410 g/mol after torrefaction at 200 and 225 °C. However, the M_w slightly increased to 2730 g/mol in 250-MWL, which was probably related to the higher content of carbon–carbon structures (β-β and β-1) in these samples (Table 2). This suggested that the condensation reaction is dominant reaction at this temperature. By contrast, due to the absence of the frequent linkages (β-*O*-4, β-β, and β-1), the M_w decreased to 2130 and 1560 g/mol as resulted of cleavage and depolymerisation reaction at harsh temperatures (275 and 300 °C).

4. Conclusions

The physical and chemical characteristics of the torrefied bamboo at different temperatures (200–300 °C) have been investigated. The results showed that torrefaction at 275 °C for 1 h is the optimal condition to prepare torrefied bamboo. The energy yield reached to 85.7% of initial energy content, while the mass yield is 70.1% at this temperature. During torrefaction, the changes of hemicelluloses, cellulose, and lignin occurred, such as degradation of hemicelluloses, crystalline transformation and degradation of cellulose, structural changes of lignin macromolecules. The chemical and structural transformations of lignin induced by torrefaction were thoroughly studied in this study. The comprehensive NMR results indicated that aryl-ether bonds (β-*O*-4) and *p*-CE in lignin were cleaved during the torrefaction process. The fragmentation, depolymerisation, condensation and demethoxylation reactions also occurred accompanying with the cleavages of the main linkages in lignin. The severe treatments of bamboo (275 and 300 °C) induced a dramatic enrichment in lignin content together with the almost complete disappearance of β-*O*-4, β-β, and β-5 linkages. It is believed that the understanding the reactivity and chemical transformations of lignin macromolecules during torrefaction will contribute to study the integrated torrefaction mechanism and maximize the energy from bamboo biomass.

Acknowledgements

This work was supported by financial support from National Science Foundation of China (31110103902), Major State Basic Research Projects of China (973-2010CB732204), and State Forestry Administration (20124803).

Appendix A. Supplementary material

Supplementary data associated with this article can be found, in the online version, at http://dx.doi.org/10.1016/j.apenergy.2014.02.001.

References

[1] Tran K-Q, Luo X, Seisenbaeva G, Jirjis R. Stump torrefaction for bioenergy application. Appl Energy 2013;112:539–46.

[2] Van der Stelt M, Gerhauser H, Kiel J, Ptasinski K. Biomass upgrading by torrefaction for the production of biofuels: A review. Biomass Bioenerg 2011;35:3748–62.

[3] Wannapeera J, Worasuwannarak N. Upgrading of woody biomass by torrefaction under pressure. J Anal Appl Pyrol 2012;96:173–80.

[4] Shang L, Ahrenfeldt J, Holm JK, Sanadi AR, Barsberg S, Thomsen T, et al. Changes of chemical and mechanical behavior of torrefied wheat straw. Biomass Bioenerg 2012;40:63–70.

[5] Rousset P, Macedo L, Commandré JM, Moreira A. Biomass torrefaction under different oxygen concentrations and its effect on the composition of the solid by-product. J Anal Appl Pyrol 2012;96:86–91.

[6] Park S-W, Jang C-H, Baek K-R, Yang J-K. Torrefaction and low-temperature carbonization of woody biomass: evaluation of fuel characteristics of the products. Energy 2012;45:676–85.

[7] Chen W-H, Cheng W-Y, Lu K-M, Huang Y-P. An evaluation on improvement of pulverized biomass property for solid fuel through torrefaction. Appl Energy 2011;88:3636–44.

[8] Wu K-T, Tsai C-J, Chen C-S, Chen H-W. The characteristics of torrefied microalgae. Appl Energy 2012;100:52–7.

[9] Chen W-H, Lu K-M, Tsai C-M. An experimental analysis on property and structure variations of agricultural wastes undergoing torrefaction. Appl Energy 2012;100:318–25.

[10] Chen W-H, Kuo P-C. Torrefaction and co-torrefaction characterization of hemicellulose, cellulose and lignin as well as torrefaction of some basic constituents in biomass. Energy 2011;36:803–11.

[11] Rousset P, Aguiar C, Labbé N, Commandré J-M. Enhancing the combustible properties of bamboo by torrefaction. Bioresour Technol 2011;102:8225–31.

[12] Zheng A, Zhao Z, Chang S, Huang Z, Wang X, He F, et al. Effect of torrefaction on structure and fast pyrolysis behavior of corncobs. Bioresour Technol 2013;128:370–7.

[13] Kim Y-H, Lee S-M, Lee H-W, Lee J-W. Physical and chemical characteristics of products from the torrefaction of yellow poplar (*Liriodendron tulipifera*). Bioresour Technol 2012;116:120–5.

[14] Ibrahim R-H, Darvell L-I, Jones J-M, Williams A. Physicochemical characterisation of torrefied biomass. J Anal Appl Pyrol 2013;103:21–30.

[15] Melkior T, Jacob S, Gerbaud G, Hediger S, Le Pape L, Bonnefois L, et al. NMR analysis of the transformation of wood constituents by torrefaction. Fuel 2012;92:271–80.

[16] Scurlock J, Dayton D, Hames B. Bamboo: an overlooked biomass resource? Biomass Bioenerg 2000;19:229–44.

[17] Wen J-L, Sun S-L, Xue B-L, Sun R-C. Quantitative structural characterization of the lignins from the stem and pith of bamboo (*Phyllostachys pubescens*). Holzforschung 2013;67:613–27.

[18] Weiland J, Guyonnet R, Gibert R. Analysis of controlled wood burning by combination of thermogravimetric analysis, differential scanning calorimetry and Fourier transform infrared spectroscopy. J Therm Anal 1998;51:265–74.

[19] Rousset P, Lapierre C, Pollet B, Quirino W, Perre P. Effect of severe thermal treatment on spruce and beech wood lignins. Ann Forest Sci 2009;66:110–7.

[20] Ralph J, Landucci L-L. NMR of lignins. In: Lignin and lignans: advances in chemistry. CRC Press; 2010. p. 137–244.

[21] Wen J-L, Sun S-L, Xue B-L, Sun R-C. Recent advances in characterization of lignin polymer by solution-state nuclear magnetic resonance (NMR) methodology. Materials 2013;6:359–91.

[22] Pu Y, Cao S, Ragauskas A-J. Application of quantitative ^{31}P NMR in biomass lignin and biofuel precursors characterization. Energ Environ Sci 2011;4:3154–66.

[23] Faravelli T, Frassoldati A, Migliavacca G, Ranzi E. Detailed kinetic modeling of the thermal degradation of lignins. Biomass Bioenerg 2010;34:290–301.

[24] Björkman A. Isolation of lignin from finely divided wood with neutral solvents. Nature 1954;174:1057–8.

[25] Wen J-L, Xue B-L, Xu F, Sun R-C, Pinkert A. Unmasking the structural features and property of lignin from bamboo. Ind Crops Prod 2013;42:332–43.

[26] Sluiter A, Hames B, Ruiz R, Scarlata C, Sluiter J, Templeton D, et al. Determination of structural carbohydrates and lignin in biomass. Laboratory Analytical Procedure (NERL); 2008.

[27] Liu H-M, Feng B, Sun R-C. Acid-chlorite pretreatment and liquefaction of cornstalk in hot-compressed water for bio-oil production. J Agric Food Chem 2011;59:10524–31.

[28] Wen J-L, Sun Y-C, Meng L-Y, Yuan T-Q, Xu F, Sun R-C. Homogeneous lauroylation of ball-milled bamboo in ionic liquid for bio-based composites production Part I: modification and characterization. Ind Crops Prod 2011;34:1491–501.

[29] Wen J-L, Sun S-L, Xue B-L, Sun R-C. Quantitative structures and thermal properties of the birch lignins after ionic liquid-based biorefinery. J Agric Food Chem 2013;61:635–45.

[30] Crestini C, Argyropoulos D-S. Structural analysis of wheat straw lignin by quantitative ^{31}P and 2D NMR spectroscopy. The occurrence of ester bonds and α-O-4 substructures. J Agric Food Chem 1997;45:1212–9.

[31] Prins M-J, Ptasinski K-J, Janssen F-J. Torrefaction of wood: Part 1. Weight loss kinetics. J Anal Appl Pyrol 2006;77:28–34.

[32] Sannigrahi P, Kim D-H, Jung S, Ragauskas A. Pseudo-lignin and pretreatment chemistry. Energy Environ Sci 2011;4:1306–10.

[33] Wallace G, Russell W-R, Lomax J-A, Jarvis M-C, Lapierre C, Chesson A. Extraction of phenolic-carbohydrate complexes from graminaceous cell walls. Carbohydr Res 1995;272:41–53.

[34] Ben H, Ragauskas AJ. Torrefaction of loblolly pine. Green Chem 2012;14:72–6.

[35] Faix O. Classification of lignins from different botanical origins by FT-IR spectroscopy. Holzforschung 1991;45:21–8.

[36] Nimz H, Robert D, Faix O, Nemr M. Carbon-13 NMR spectra of lignins, 8. Structural differences between lignins of hardwoods, softwoods, grasses and compression wood. Holzforschung 1981;35:16–26.

[37] Granata A, Argyropoulos D. S. 2-Chloro-4, 4, 5, 5-tetramethyl-1, 3, 2-dioxaphospholane, a reagent for the accurate determination of the uncondensed and condensed phenolic moieties in lignins. J Agric Food Chem 1995;43:1538–44.

[38] Yuan T-Q, Sun S-N, Xu F, Sun R-C. Structural characterization of lignin from triploid of Populus tomentosa Carr. J Agric Food Chem 2011;59:6605–15.

[39] Nicolas B, Roland E-H, Mounir C, Mathieu P, Stéphane D, Philippe G. Investigation of the chemical modifications of beech wood lignin during heat treatment. Polym Degrad Stabil 2010;95:1721–6.